Characterizing and Testing a Thermally Isolating Superconducting Link for SAFIRE-Like Missions

Final Report

Principal Investigators: Dr. Raouf R. Selim and Dr. Randall Caton
Department of Physics and Computer Science

Period: March 26, 1991 through June 30,1995

CHRISTOPHER NEWPORT UNIVERSITY
NEWPORT NEWS, VIRGINIA 23606-2998

NASA Research Grant NUMBER NAG-1-1242

November 10, 1995

Introduction

The discovery of a new class of ceramic superconductors with transition temperatures above the boiling point of liquid nitrogen has opened the doors for several space applications. One important space application is the fabrication of an electrically conducting and thermally isolating link to replace manganin wires used in connecting IR detectors to data acquisition electronics on remote sensing platforms like SAFIRE and SIRTF. These NASA platforms designed to monitor the earth's atmosphere from space use infrared detectors which operate at liquid helium temperature (4.2K) for optimum performance. The SAFIRE mission employs hybrid dewars which combine both mechanical and cryogenic liquid cooling. The lifetime of such a mission is limited by the heat conducted through sensor array leads that connect the electronics (at ~ 80 K) to the sensors (at ~ 4 K). Currently these remoter sensing systems use manganin wires to connect the IR detectors to the data acquisition electronics. This link between a detector operating at 4 K and electronics operating at 80 K must be made of material that has high electrical conductivity and high thermal resistance. The YBCO superconductor with a transition temperature, T_c, of 93 K can achieve these conflicting requirements. A link with these characteristics will improve the thermal isolation of IR detectors and will increase the lifetime of the cryogen. The fabrication of an electrically conducting and thermally isolating link that replaces the manganin wires is an important application that will improve thermal isolation of IR detectors and will increase the lifetime of the cryogen. The link is made by screen printing superconducting lines on a low thermal conductivity ceramic substrate. Developing, modeling, and testing this high temperature superconducting link is a collaborative effort among NASA-Langley Research Center, Christopher Newport University (CNU), Clemson University and the industrial companies that have joined the Commercialization of Space Program for the purpose of developing and testing this link.

CNU's effort in the development of this superconducting link included the following major efforts:

(1) Development of a thermal conductivity measurement system for high temperature superconductors and ceramic materials which are potential candidates for use as substrates in this link.

(2) Development of a mathematical model for the superconducting link that studies the effect of materials and geometry on the heat load and life time of missions.

(3) Characterization of high T_c materials and assemblies made for space applications. Properties studied include humidity effects and aging effects on high Tc materials.

This report summarizes the results of the research studies that were completed. Copies of publications detailing these findings are attached to this report.

1) Development of a thermal conductivity measurement system for high temperature superconductors and ceramic materials.

We have developed apparatus for measurement of thermal conductivity in the temperature range of 15-120K for solid materials with low thermal conductivity using a longitudinal steady-state technique. This experimental method is suitable for measuring the thermal conductivity of superconducting and insulating materials that are candidates for use as conductors and substrates for the screen-printed superconducting link. These measurements are crucial to the characterization of a superconducting link, which should ideally have a very low thermal conductivity.

We have used a He closed cycle refrigerator, where the sample length is limited to a maximum of 2 cm. One end of the sample is clamped to the cold tip of the refrigerator and a heater is wound on the free end of the sample. A radiation shield, kept at temperature close to the sample temperature, was used to cut down on the heat loss by radiation. The temperature gradient along the sample was measured using a type-E differential thermocouple and the temperature of the sample was measured using a platinum resistance thermometer.

A. Experimental Details

Samples are cut into rectangular bars 1-2.5 mm thick, 4-6 mm wide (cross section area, A, of 4-15 mm^2) and 15-20 mm long. Two holes - each 0.5 mm in diameter - are drilled in the sample with a separation, L, of 3-4 mm (see figure 1.) The beads of a type-E (Nickel-10%Chromium & Constantan) differential thermocouple are inserted in the holes and glued in place using GE-7031 varnish to provide good thermal contact with the sample in order to measure the temperature drop in the longitudinal direction. A heater made of 25 μm diameter constantan wire is wrapped around the free end of the sample with a resistance value of 100-200

ohms. The top of the sample is fastened to the cold tip of the refrigerator using a clamp in a specially designed copper attachment. The sample is put in good thermal contact with the cold tip by using the GE-7031 varnish. A platinum resistance thermometer to measure the sample temperature and a thin film resistive heater to control the temperature of the set up are mounted on the copper attachment at the top of the sample. To cut down on the heat loss by radiation, a cylindrical shield made of copper is attached to the top of the assembly by four screws. The volume surrounded by the sample is kept at pressure of 10^{-5} torr or less during the measurement to minimize the heat loss by conduction.

B. Data Acquisition and Instrumentation

The data acquisition system developed for the measurement is a fully automated one. We use an HP 300 series computer to control all the measuring instruments via the IEEE-488 parallel interface bus. The schematic diagram of the data acquisition system is shown in figure 2.

The power delivered to the sample heater is measured using a 4-probe technique. The current, I, to the sample heater is supplied by a Keithley 220 constant current source and the voltage across the heater, V, is measured using an HP 3456A digital voltmeter. The voltage across the type-E differential thermocouple is measured by a Keithley 181 nanovoltmeter and converted to temperature difference, ΔT. The sample temperature is measured by a Lake Shore DRC-82C temperature controller using a platinum resistance thermometer. When the sample temperature is stable within ± 0.1K, the program starts monitoring the differential thermocouple voltage and calculates the change of ΔT with time. If the drift of ΔT is less than ± 0.5 mK/s, the program calculates an average value, ΔT_1, for the temperature difference along the sample and then the heater current is started. After a wait period of 6-12 minutes, to allow for the sample to reach thermal equilibrium, the temperature difference along the sample, ΔT_2, is calculated. The thermal conductivity, k, is then calculated from the heat power equation:

$$Q = I V = k A \Delta T / L$$

where I is the heater current, V is the heater voltage, A is the cross section area of the sample, L is the separation between the differential thermocouple beads, and $\Delta T = \Delta T_2 - \Delta T_1$. After a successful measurement of K at a certain temperature, the LakeShore temperature controller is used to raise the temperature of the setup by 1 - 2 K to a higher temperature. The sample temperature is monitored until it is stable within ±0.1 K before attempting to measure k again. The software developed allows for changing many control parameters during the experiment, which is necessary to do at different stages of the measurement. Some of these parameters are: the desired temperature gradient along the sample (typically 1- 1.5K), the acceptable drift value of ΔT, and the wait time after the heater current is applied.

C. RESULTS

In Fig. 3 the improvement of the thermal conductivity measurement through several modifications of the experiment is indicated by the progression towards the accepted value for fused silica. The measurement (FS3_R5) shows excellent agreement with the accepted value and is reproducible in different trials. The improvements that have contributed the most to more accurate results are:

1) the reduction of the diameter of the thermocouple wire used for the differential temperature measurement and the use of constantan wires to carry current to the sample heater in order to reduce heat conduction to the sample through these wires.
2) the measurement of the voltage across the sample heater.
3) improved bonding of the heater to the thermal sink.
4) improvement of the sample geometry.

We can now make thermal conductivity measurements reliable to 5% in a very convenient to use closed cycle refrigerator in a small sample space.

One of the candidates for substrate material for the link is yttria stabilized zirconia (YSZ). Results of measurements on two samples provided by NASA (closed square and open diamonds) appear in Fig. 4 along with previous measurements from the literature (open squares and closed diamonds). The two upper curves show data for the tetragonal phase, while the two lower show data for the cubic phase.

It is clear that the cubic phase is preferred due to its lower thermal conductivity and that it is necessary to measure the material that will actually be used rather than rely on literature values.

We have also measured the thermal conductivity of the superconducting phase of YBaCuO material (123 phase), and the non-superconducting (211) green phase to investigate the possibility of using this insulating material in a multi-layer link. Over 30 different superconducting samples were measured in the temperature range of 15 - 120 K.

2) Development of a model for the superconducting link Introduction

The electronic link connecting cryogenically cooled radiation detectors to data-acquisition and signal-processing electronics at higher temperatures contributes significantly to the total heat load on spacecraft cooling systems that use combined mechanical and cryogenic liquid cooling. Using high transition temperature superconductors for this link has been proposed to increase the lifetime of space missions. We examined several $YBa_2Cu_3O_7$ (YBCO or 123) and $Bi_2Sr_2Ca_2Cu_3O_x$ (BSCCO or 2223) superconductor-substrate combinations and compare total heat loads to manganin wire technology in current use. Using numerical solutions to the heat-flow equations, we demonstrate that replacing manganin technology with high temperature superconductors made by thick film technology can extend a seven year mission by up to one year.

We considered and studied some of the principles that needed to be addressed in order to develop a high T_c superconducting link for use in IR remote sensing platforms. Using SAFIRE as an example of a cryogenically cooled remote sensing atmospheric mission that requires an electrically conducting and thermally isolating link connecting a detector at 4 K to electronics at 80 K, we note the following differences between conventional and superconducting links:

1. The state-of-the-art technology of conventional wires uses 158 manganin wires encased in Kapton ribbon. These 40 AWG manganin wires are approximately 6 inches long, with a 0.1 mil shield. For SAFIRE this conventional link produces 33 % of the instrument heat load on the liquid cryogen or 17% of the total heat load.

2. The state-of-the-art superconducting thick film technology produces $YBa_2Cu_3O_x$ (YBCO or 123) and $Bi_2Sr_2Ca_2Cu_3O_x$ (BSCCO or 2223) wires made by the screen printing process. Wires are 2-3 mils (50-75 microns) in width at a 2-3 mil spacing, and 20-25 micron in thickness with a reduced cross sectional area of ~ 1000-1500 μm^2 per wire. Such wires are printed on MgO, Al_2O_3, or YSZ (Y_2O_3-stabilized ZrO_2) substrates.

Using such high T_C material can result in a significant reduction of the heat load from the link.

A. Theory

We have investigated the effect of different parameters on the performance of the link: wire material, cross sectional area per wire, substrate material, and the thickness of the substrate.

We need to describe the heat transport in one dimension between two isolated thermal reservoirs, one at a high temperature T_H and and the other at a lower temperature T_L , linked by an element which has a thermal conductivity K and an electrical resistivity ρ_{elect} as shown in Figure 5. Heat flows from the high temperature reservoir to the low temperature reservoir and, in addition, when an electrical current flows through the element, heat is generated along its length.

Assuming that the heat flow occurs only in the direction of the linking element we obtain the heat flow equation

$$\frac{\partial}{\partial t}(\rho c T) - \frac{\partial}{\partial x}\left(K\frac{\partial T}{\partial x}\right) = J^2\rho_{elect}$$

Of course, in this expression the specific heat c, the thermal conductivity K, and the electrical resistance ρ_{elect} are functions of temperature.

We are mainly interested in the steady state behavior of the linking system which is governed by the following ordinary differential equation

$$\frac{d}{dx}\left[K(T)\frac{dT}{dx}\right] = -J^2\rho_{elect}(T) .$$

It is instructive to solve this equation first assuming that the thermal conductivity and electrical resistivity do not change with temperature; in this case the exact solution has the form

$$T(x) = T_L + (T_H - T_L)\frac{x}{L} - \frac{J^2 \rho_{elec}}{2K}\left(x^2 - xL\right).$$

The first two terms give the linear behavior of the thermal gradient contribution while the third term gives the contribution from the the electrical power dissipation in the link. Any further contributions to the spatial dependence of the temperature distribution are due to changes in the thermal conductivity with temperature. When the thermal conductivity and electrical resistance vary with temperature we must employ numerical techniques to determine the temperature distribution in the wire.

B. Calculation

Numerical calculations for the one-dimensional heat transfer problem were carried out using a Runge-Kutta method with MathCAD™. We have used thermal conductivity data from the literature for the following materials: manganin, YBCO, tetragonal YSZ, cubic YSZ, and amorphous silica. At low temperatures the thermal properties of the materials under consideration depend on temperature (see Figs. 3 and 4.) The temperature dependencies for the electrical resistivity and thermal conductivity were approximated by linear or quadratic functions. It was found that the Joule heating was insignificant at the low current densities ($\leq$ 0.1 A/cm^2) required for the proposed applications. The temperature and temperature gradient at the low temperature end of the sample were input as parameters to the numerical solution of the second order differential heat transfer equation. The program was run repeatedly, choosing a new temperature gradient until the temperature at the high temperature end of the sample met the specified design value. The step size for numerical integration was continually decreased until the solution stabilized. Typically this occurred when the step size was about one thousandth of the total interval size.

C. Results

We wanted to compare manganin (#40 wire) to the various YBCO-substrate combinations and compare only the more reliable numerical results. Table 1 clearly shows that the largest contributor to the heat load for the YBCO-substrate combinations is the substrate. The film width for YBCO (which controls the substrate width per wire) and substrate thicknesses are values we feel very confident in with present technology. YBCO on any substrate represents an improvement over #40 manganin wire. The result for the YBCO-amorphous silica combination projects an increased mission lifetime of about one year for a seven year mission compared to using #40 manganin wire. The three combinations mentioned must continue to be considered because they all have advantages. Even though the YSZ substrates contribute a higher heat load, they are superior in strength and it is relatively easy to lay down thick YBCO films of high quality on YSZ substrates.

An important comment is in order. Although the numerical calculations include a Joule heating term, the results for manganin (the only normal conductor) were not affected by the Joule heating term because the current for the envisioned application is quite low (1 μA). As the cross section of the manganin decreases or the electrical current increases, the Joule heating will increase. Our numerical calculations show that the Joule heating will begin to play a role to increase the heat load as the current approaches 100 μA for #40 manganin wire. This will occur sooner for #42 manganin wire because of its smaller cross-sectional area. For higher current applications the YBCO-substrate combinations will result in lower heat loads up to the point where the critical current is exceeded (≈ 5 mA assuming currently obtainable YBCO with a critical current density of 200 A/cm^2). At this point we would require better quality thick films of YBCO.

Similar studies were done to investigate the use of $Bi_2Sr_2Ca_2Cu_3O_x$ (2223) wires made by the screen printing process. Table 2 shows the results for two models. Model 1 uses superconducting leads printed on a single side of substrate, while model 2 uses printed leads on both sides of the substrate with identical printing configurations. Figure 7 shows the geometrical configurations for both models and table 2 gives the heat load per lead. The results clearly show that all high T_c leads on fused silica or

YSZ give better heat loads than manganin wires. The most superior performance is that of 2223 Bi leads printed on fused silica. Table 3 shows how these heat loads translate into savings for space missions. On a 7 year mission, employing high Temperature superconducting leads will add up to 12 months to the life of such a mission.

D. Conclusion

We have carried out an analysis of the heat load on a cooling system that employs low-temperature detectors. This analysis shows the importance of using the numerical solution to the differential equations for one-dimensional heat flow in estimating the heat load of interconnects in planned space flight missions. This analysis became very useful in determining the material used to make the substrate as well as finding optimal dimensions of the superconducting leads and the substrate thickness in order to minimize the heat load on the cryostat. While there is little chance of reducing the heat load contribution using manganin wires, there is a good chance of obtaining considerable reduction using a YBCO-substrate or BSCCO-substrate combination. Superconductors should continue to be explored as low-current carrying interconnects for missions where the interconnect contribution to the heat load plays a predominant role in the lifetime of the mission. As the number of interconnects increases, the thick film superconducting links or superconducting fibers will be more attractive.

The results of the thermal model, that we developed to study the effect of varying the link parameters on the lifetime of a mission, are published in the NASA contractor report #4477 and in the journal Cryogenics. A copy of each is included at the end of this report.

3) Characterization of high T_C materials made for space applications

A. Aging Studies

We have measured the superconducting properties and the resistance of our contacts for six samples over a four and one-half year period. Generally, we observe no effect on T_C and only modest effects or no effect on J_C and the resistance of our contacts. The results indicate that the superconductors can hold up for considerable periods of time, which is contrary to some of the earlier reports. This is most likely due to the better quality of the material (high J_C, and sharp T_C) made at CNU since better high T_C materials do not degrade as easily as poor quality ones.

1. Superconducting Transition Temperature

For most samples T_c fluctuated within ± 1.5K of the starting value during the entire period. T_c did not change noticeably during the period of study for several samples. Some samples were observed for 4.5 years with no change in T_c within the precision of the experiment (± 0.5 K). It is clear from the results that the stability of the superconducting transition temperature is not of concern when considering future applications. In most cases the transition temperature did not change within the experimental precision.

2. Normal State Resistivity

The normalized resistivity at 290K is plotted as a function of time for a selection of samples in Fig. 8. We normalized all the sample resistivities to unity at the start of the aging study and followed the changes as time passed. There is a large difference among the various samples.

3. Critical Current Density

The trend of the data indicates that samples with higher initial J_c values degrade by a smaller percentage than those with lower J_c values. This very likely reflects the higher quality of a sample with a higher J_c value. The data indicate that additions of silver result in a small retardation of J_c aging effects. The critical current densities increased dramatically with time for electron irradiated samples.

4. Contact Resistance

Plots of the normalized contact surface resistance as a function of time appear in Figs. 9 and 10. We normalized all the contact surface resistivities to unity at the start of the aging study and followed the changes as time passed. Samples P43 and P45 are plotted separately in Fig. 9 since the contact surface resistance increased markedly after 4.5 and 4 years, respectively. Normalized plots for the most of the remaining samples appear in Fig. 10. The contact surface resistivity varies considerably for samples of similar origin.

B. Humidity studies:

We have also characterized a number of samples made at NASA Langley to study the effect of humidity on high temperature superconductors. Samples were exposed to 30%, 66%, 81%, and 100% humidity for 2, 4, and 6 weeks. We have measured the resistance versus temperature between 8 -300 K for these samples to find out the effect of humidity on the superconducting transition temperature, T_c. Figure 11 shows that T_c slightly decreases as a function of time while the humidity level is the same. Figure 12 shows that T_c markedly decreases as the humidity level increases from 30 to 66 to 81% while keeping the time of exposure the same. The results of these studies are published in NASA technical paper 3368 (September 1993). A copy of this paper is attached to the report.

List of attached publications

1. "Environmental Testing of High T_c Superconductive Thermal Isolators for Space-Borne Cryogenic Detector Systems"; Materials Research Society Symposium Proceedings, ed. by D. T. Shaw, C.C. Tsuei, T. R. Schneider, Y. Shiohara; Vol. 275, P. 831 (1992).

2. "A Comparison of Superconductor and Manganin Technology for Electronic Links used in Space Mission Applications"; NASA-Langley Contractor Report 4477, December 1992.

3. "High T_c Thermal Bridges for Space-Borne Cryogenic Infrared Detectors"; Proceedings of the World Congress on Superconductivity, September, 1992, Munich, Germany; Applied Superconductivity vol. 1 P. 1363 (1993).

4. "Room Temperature Degradation of $YBa_2Cu_3O_{7-x}$ Superconductors in Varying Relative Humidity Environments" ; NASA Technical Paper 3368 (September 1993)

5. "High T_c leads for remote Sensing Applications"; Cryogenics, Vol. 34, P.119 (1994).

Overview of the facilities at CNU

During this period we continued to build our laboratory measurement capability. With NASA Langley support, the CNU superconductivity Laboratory has grown by adding many capabilities.
A summary of our current facilities follows:

EXPERIMENTAL CAPABILITIES

Electrical Resistivity (20 - 300 K)
Electrical Resistivity (25 - 1000 °C)
ac Susceptibility (20 - 300 K)
X-ray Diffraction
Thermal Conductivity (10-120 K)

EXPERIMENTAL FACILITIES

2 Closed-cycle refrigerator (20 - 300 K)
2 fully automated data acquisition systems
486 DX2, data acquisition plug-in card and IEEE-488 board
Quadra 950, data acquisition plug-in card, IEEE-488 board and
LabVIEW data acquisition software application.
HP 382 workstation with HP-VEETEST data acquisition software application.
2 nanovoltmeters
2 Constant current sources
1 Constant voltage source
1 Lock-in amplifier
General Electric X-ray diffraction apparatus

Materials PREPARATION FACILITIES

Large Marshall Tube furnace (1400 °C) for oxygen treatment
Three Processing Ovens with flowing oxygen for final treatment
Muffle ovens for air treatment (1100 °C)
25 Ton Hydraulic Press for pelletizing (1/2", 1", 2" diameter dies)
Mixer/Mill for grinding powders

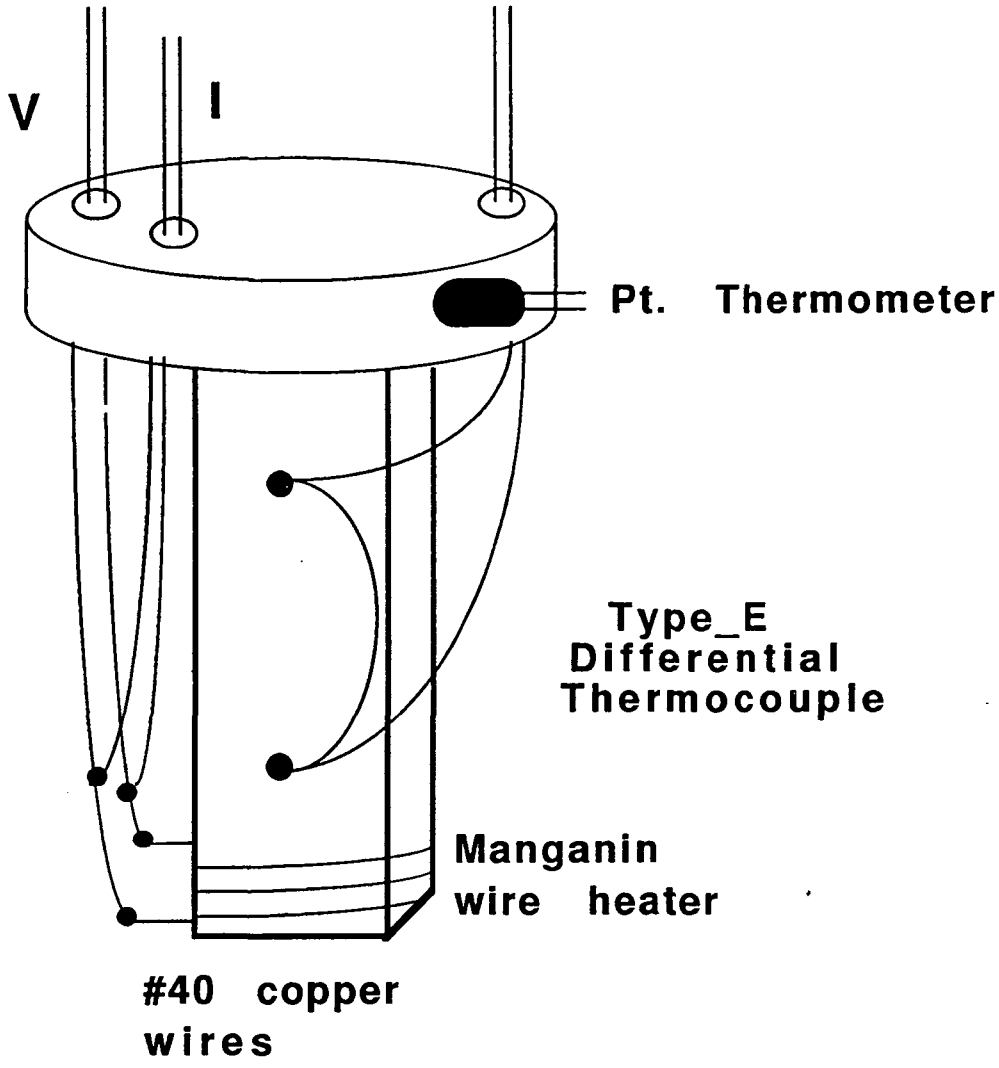

Fig. 1. Sample holder for thermal conductivity measurement.

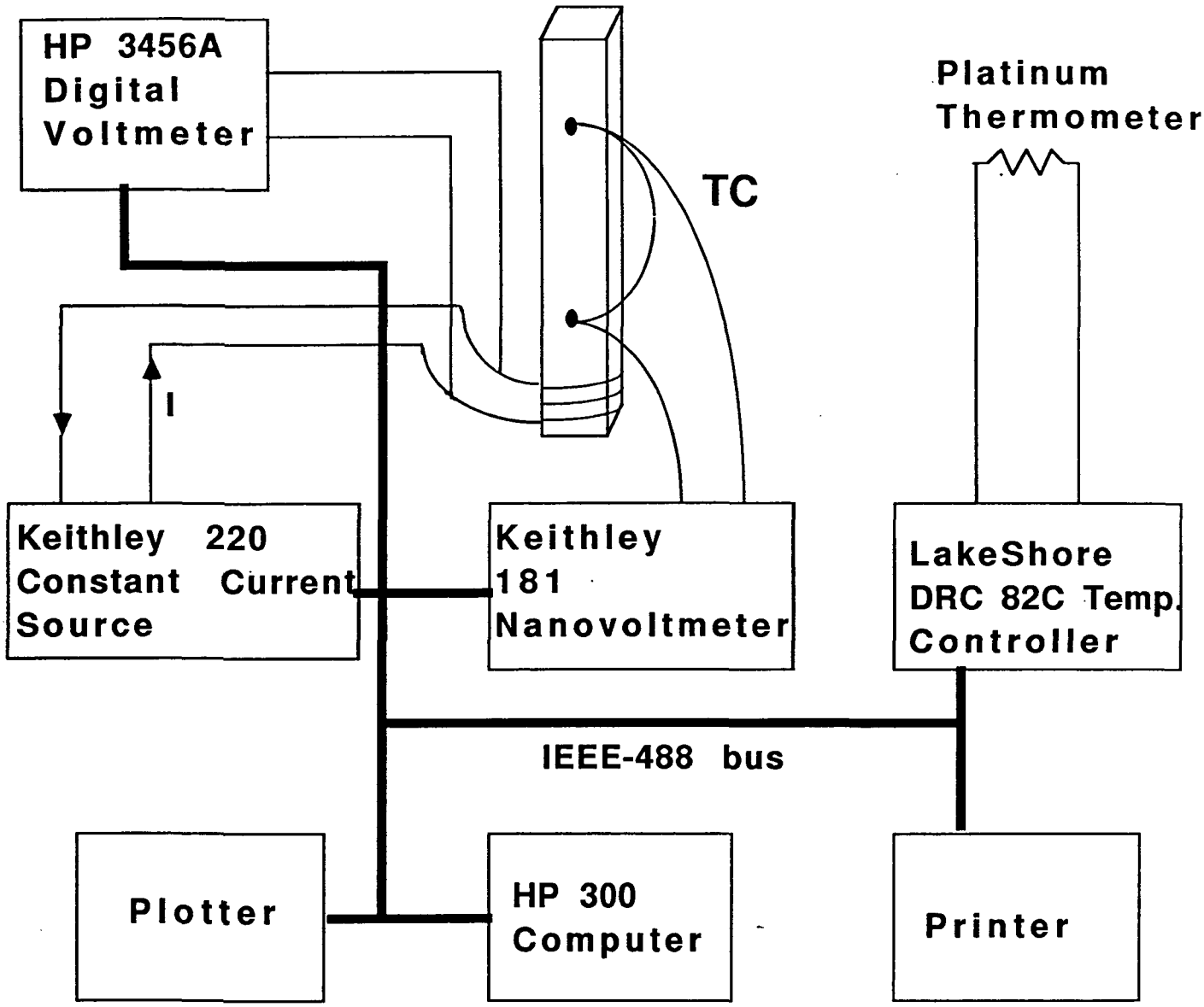

Fig. 2. Schematic diagram of the data acquisition system for thermal conductivity measurement.

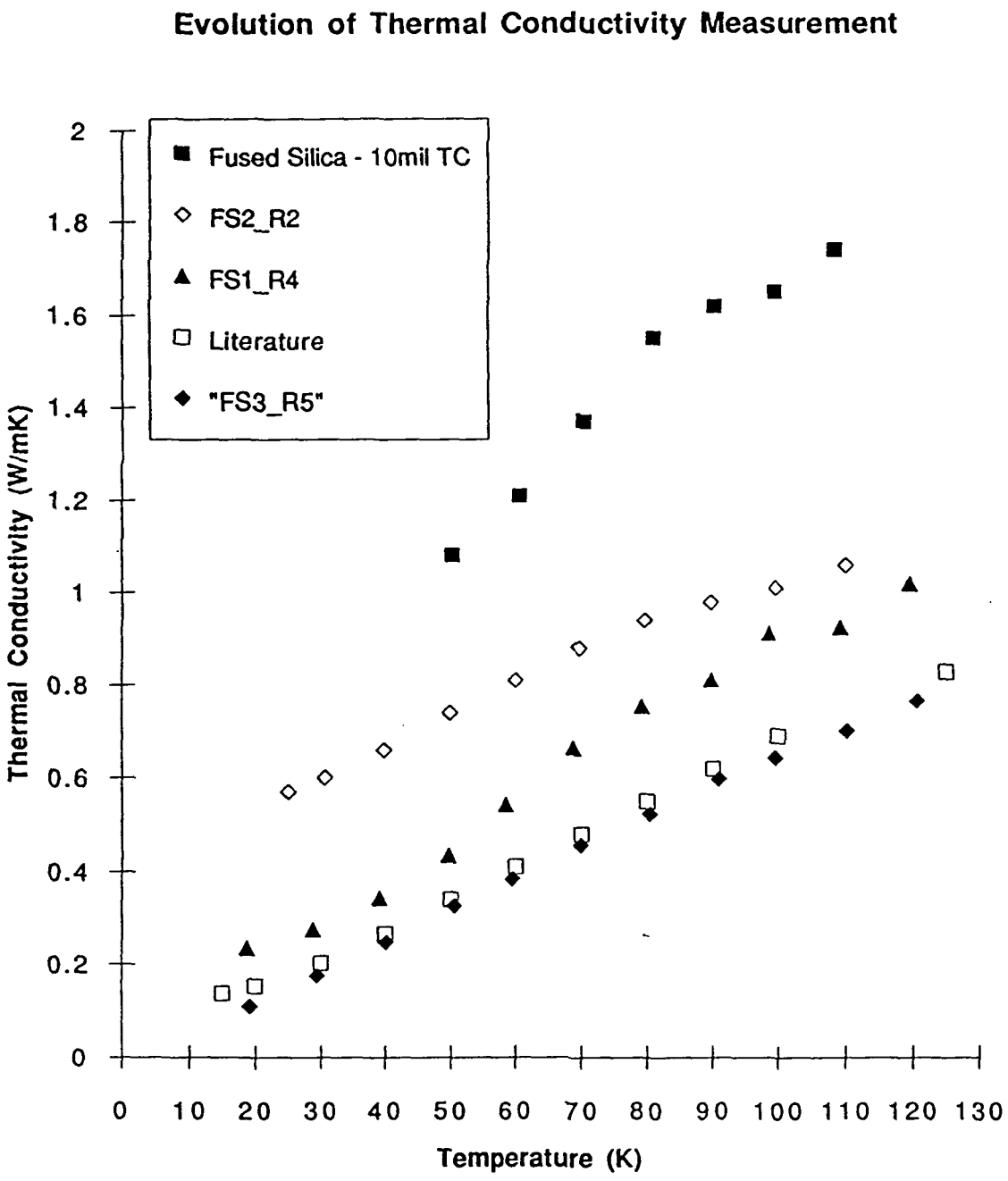

Fig. 3. Evolution of thermal conductivity measurement.

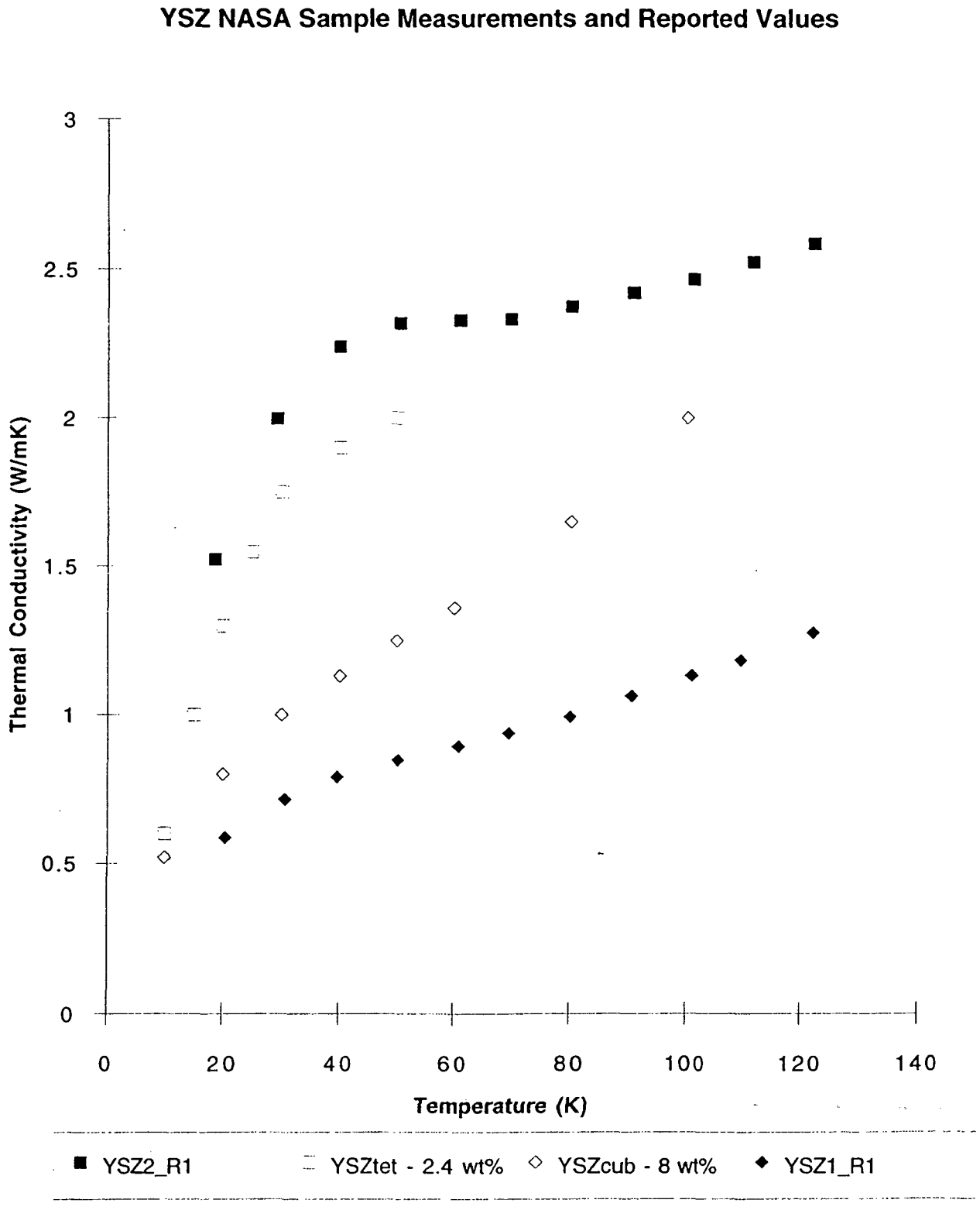

Fig. 4 YSZ measurements and reported values.

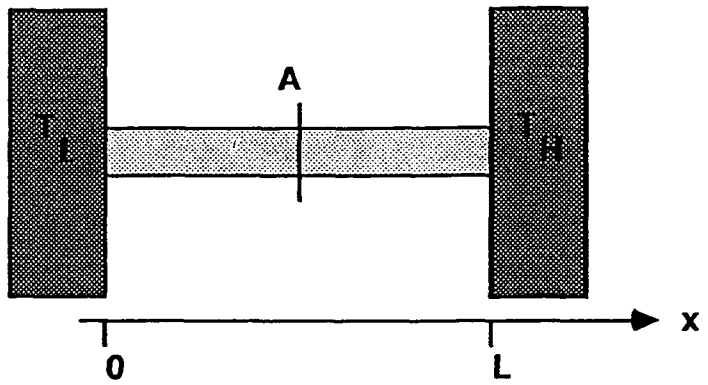

Fig. 5 Schematic diagram of the link with important parameters indicated: T_L - temperature of the lower temperature reservoir (detector), T_H -temperature of the higher temperature reservoir (electronics), A - cross-sectional area of the link, and L - length of the link.

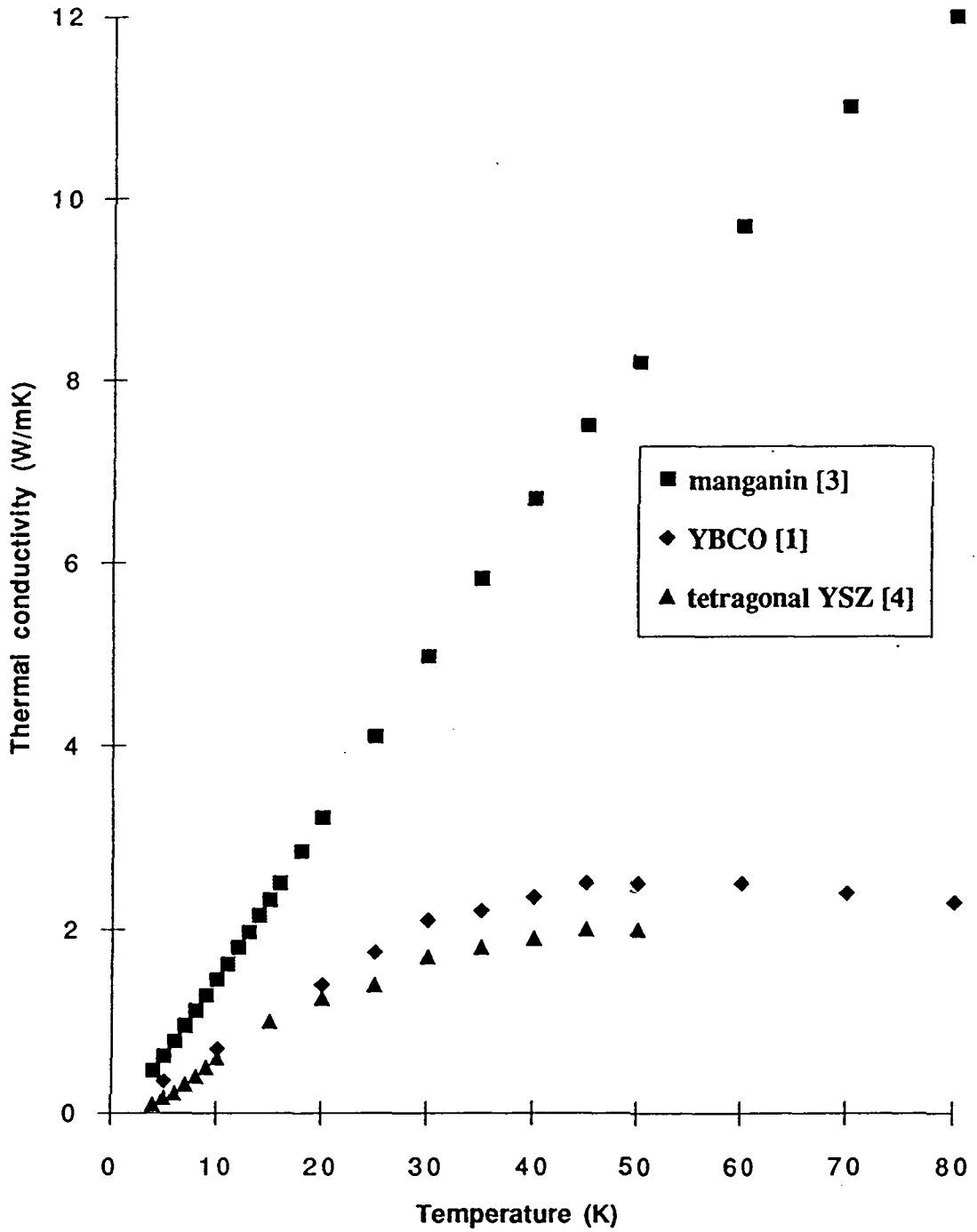

Fig. 6 Thermal conductivity *vs* temperature for various materials. Manganin - squares, YBCO - diamonds, and tetragonal YSZ - triangles.

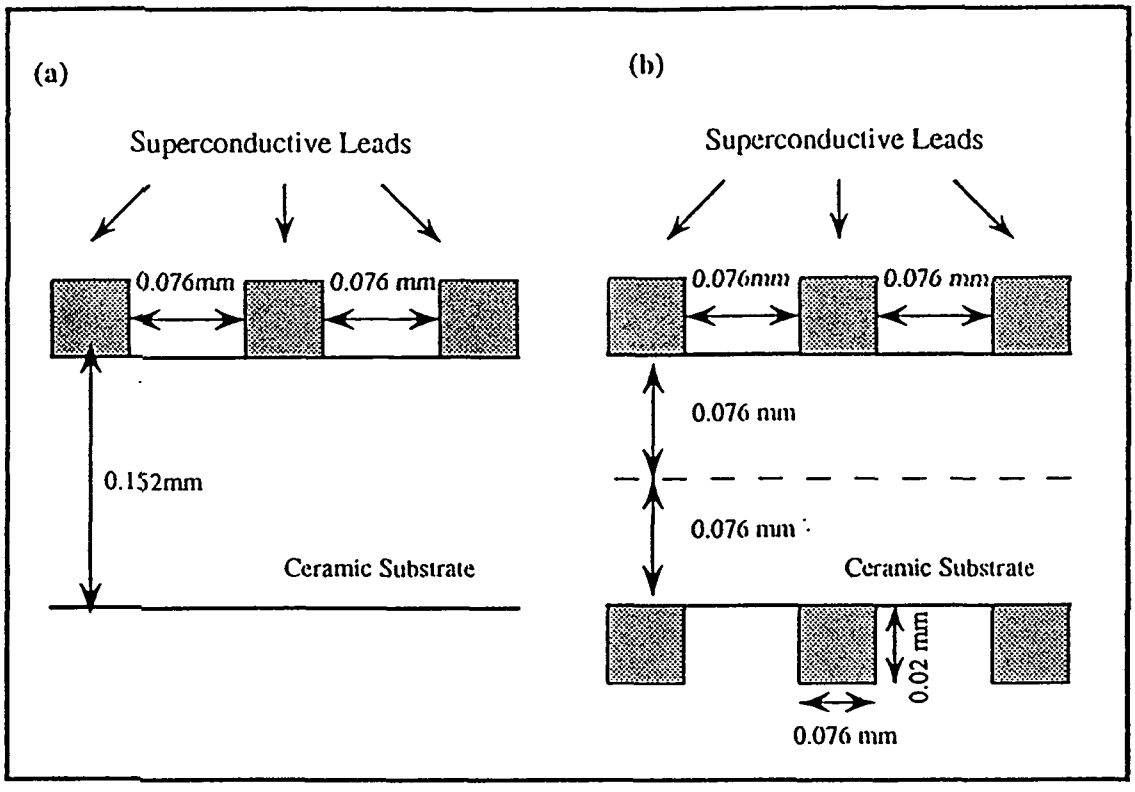

Fig. 7 Printing configurations for superconductive leads printed on (a) a single side of the substrate and (b) both sides of the substrate.

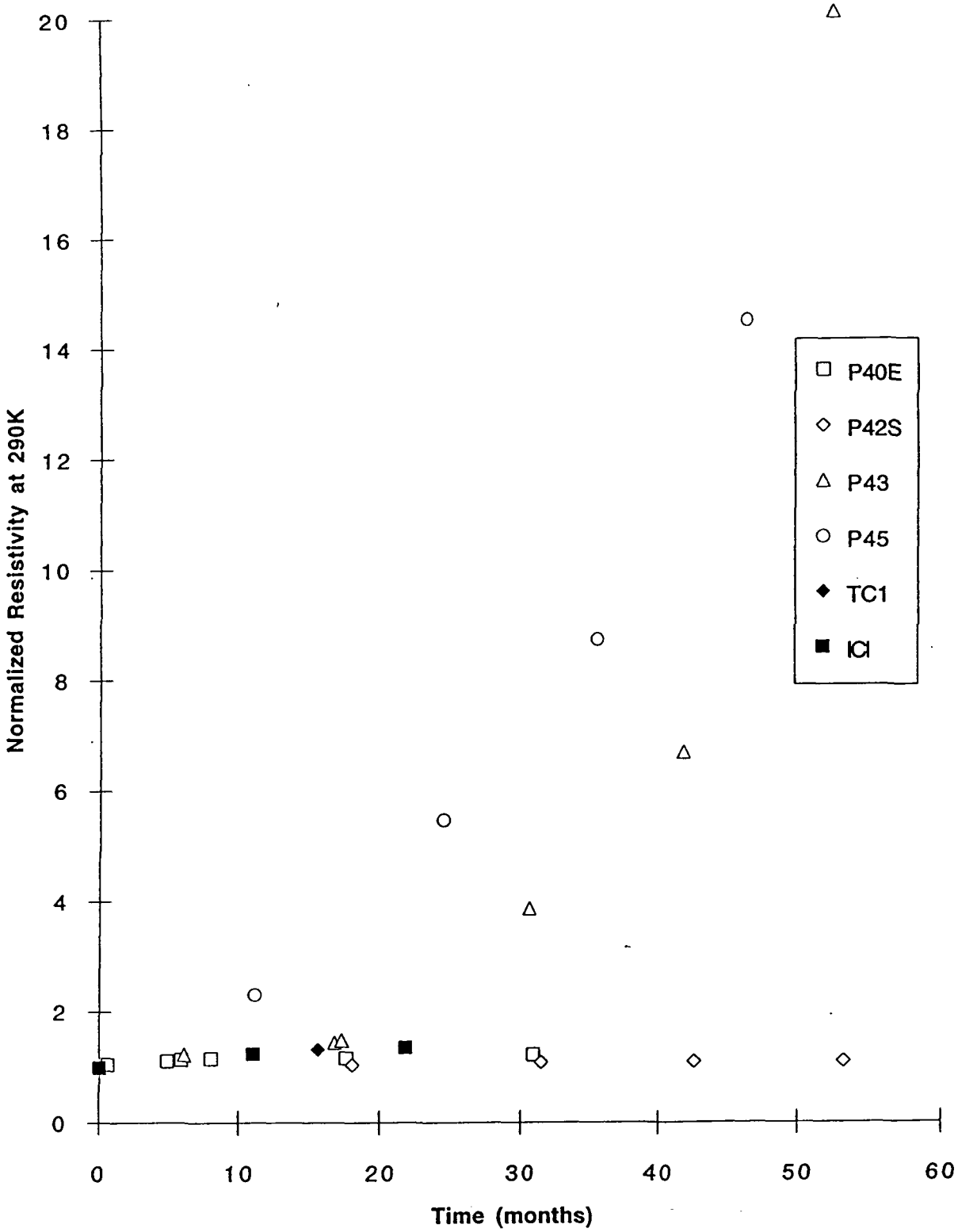

Fig. 8 Normalized resistivity at 290K as a function of time for a selection of samples.

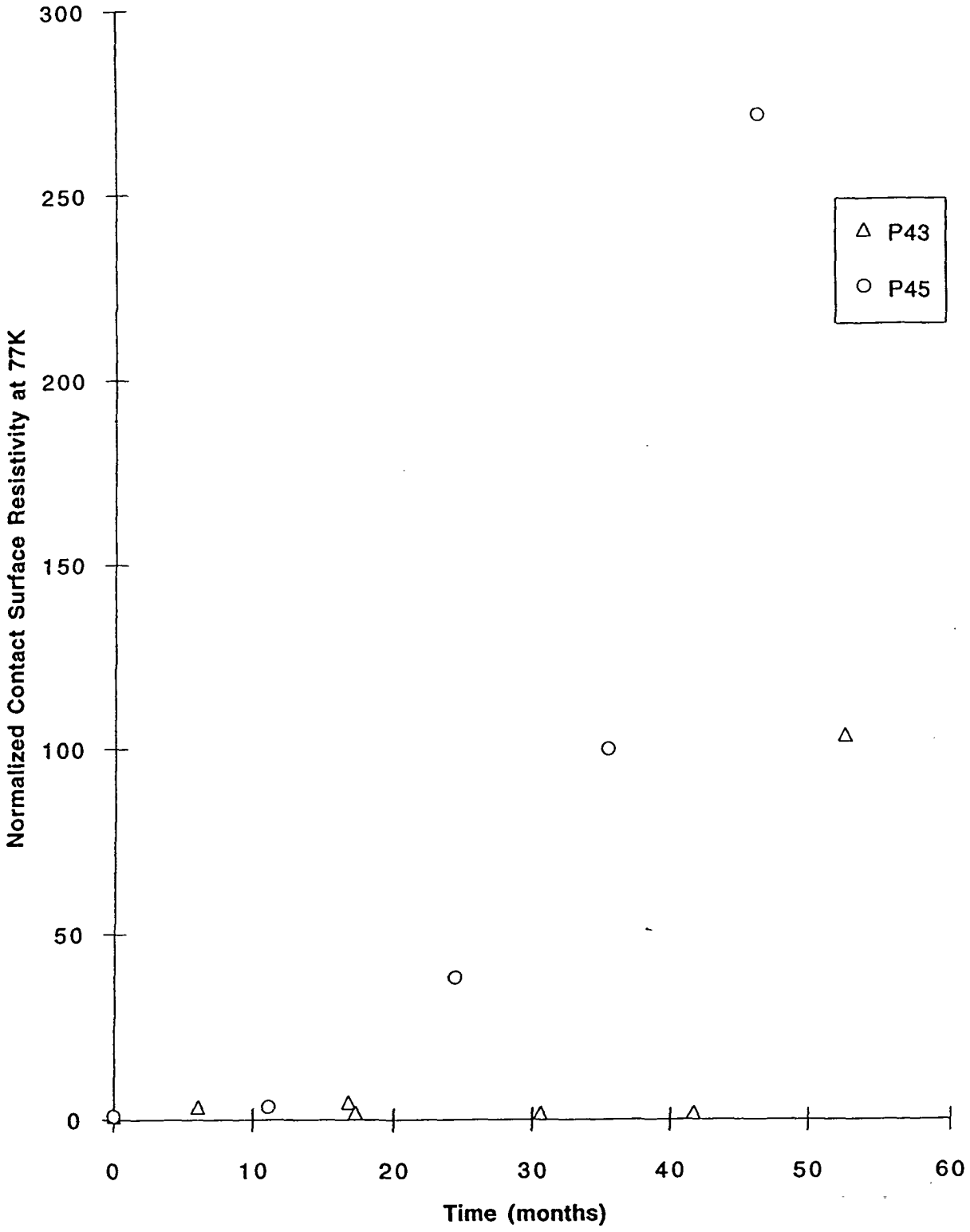

Fig. 9 Normalized contact surface resistance at 77K as a function of time for two samples.

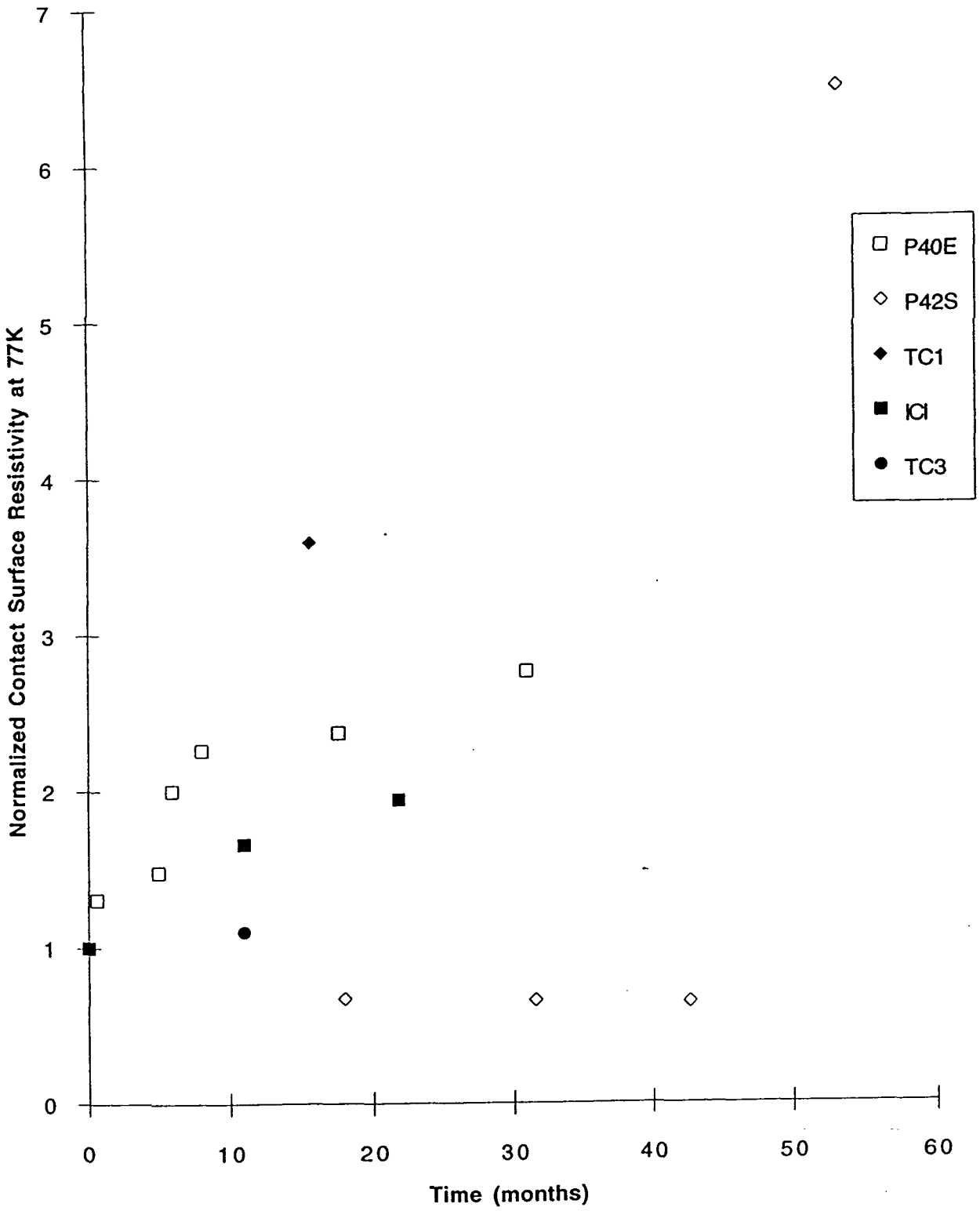

Fig. 10 Normalized contact surface resistance at 77K as a function of time for some samples.

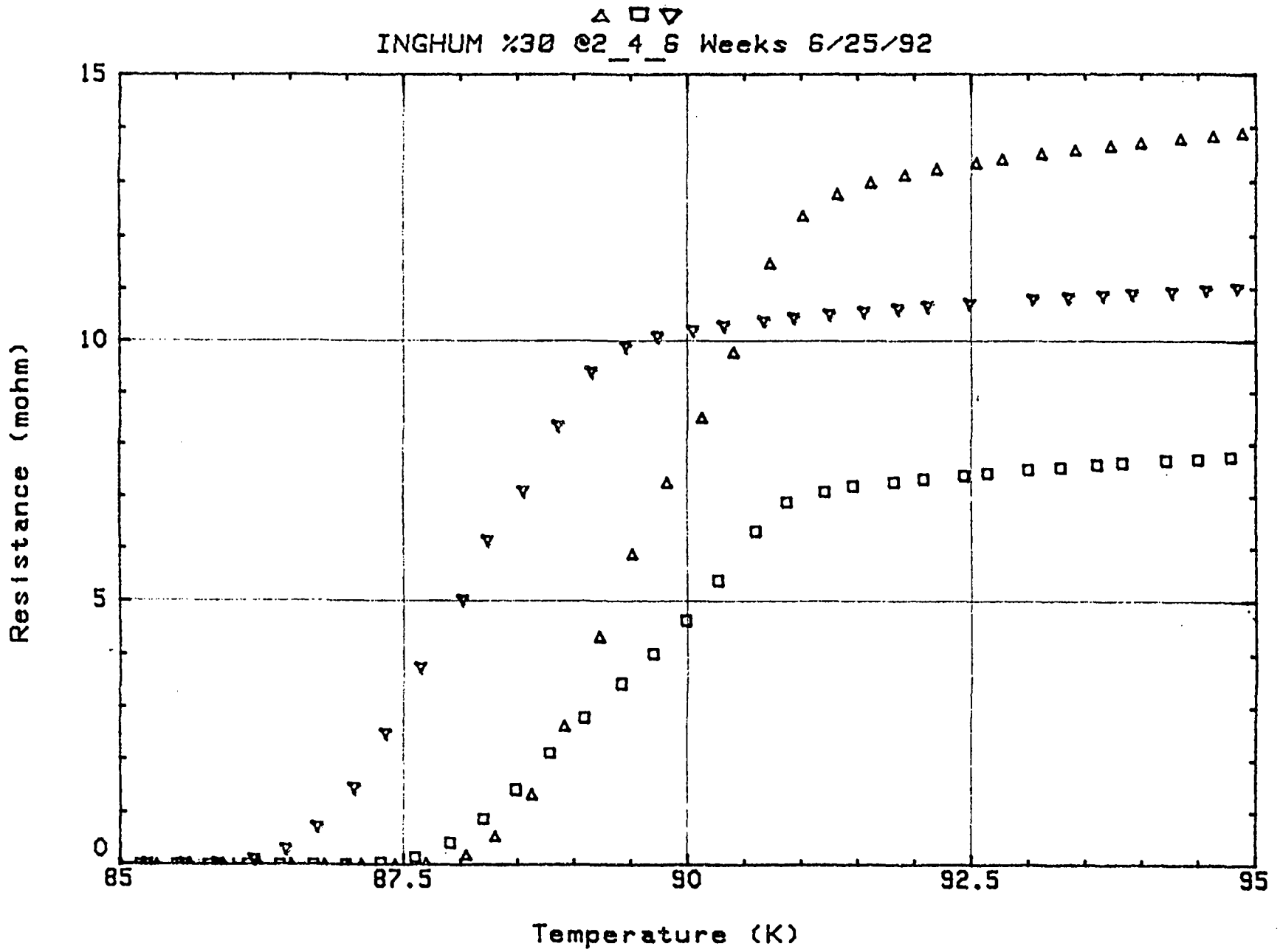

Fig. 11 Resistance versus temperature for samples exposed to 30% humidity for 2,4 and 6 weeks.

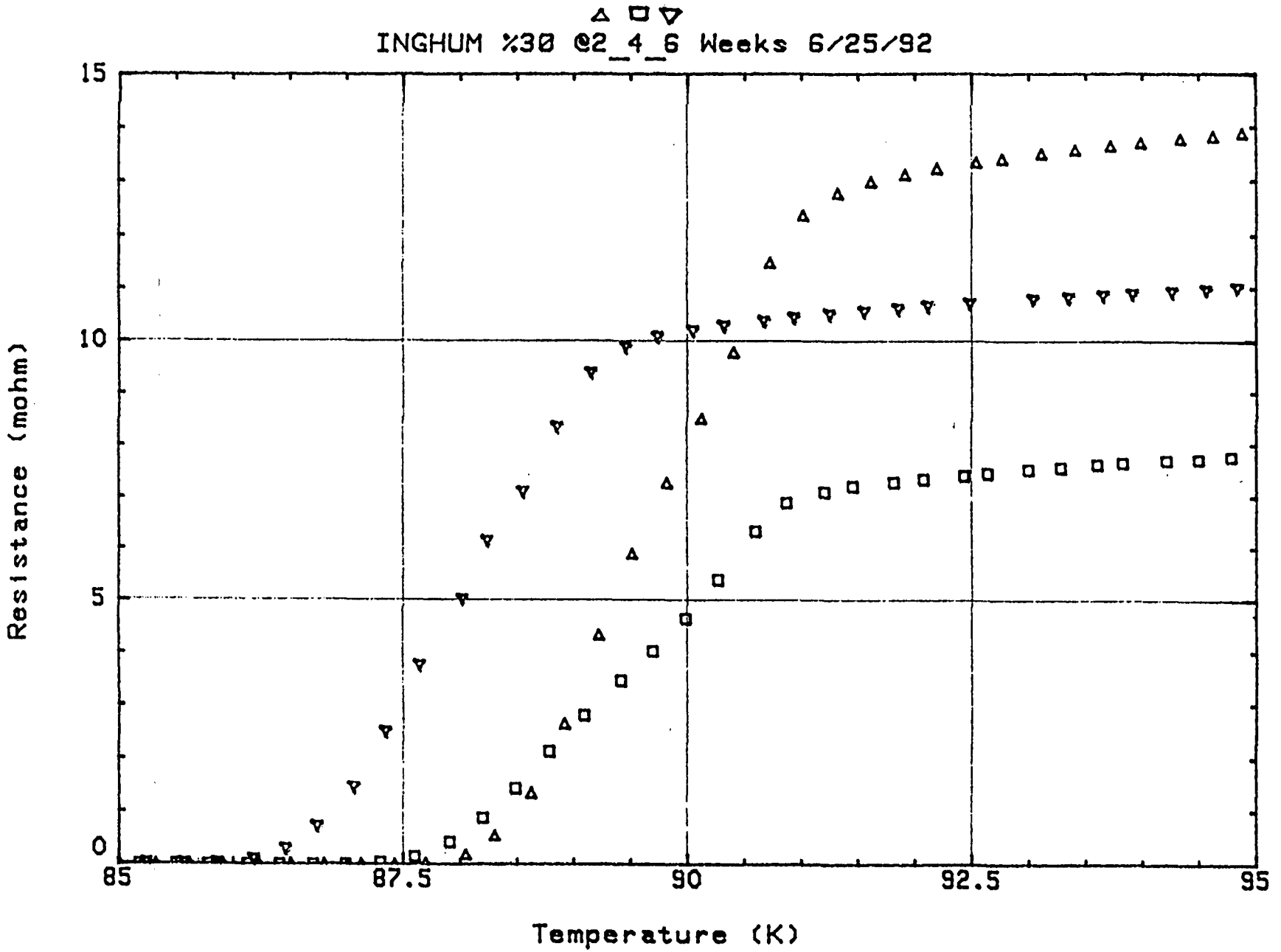

Fig. 12 Resistance versus temperature for samples exposed to 30%, 66% and 81% humidity for 2 weeks.

Material	H_{80} numerical calculation
Manganin #40	16.6
$YBa_2Cu_3O_7$ *	1.3
YSZ tetragonal **	12.5
Total 1	13.8
$YBa_2Cu_3O_7$ *	1.3
YSZ cubic **	8.5
Total 2	9.8
$YBa_2Cu_3O_7$ *	1.3
a-SiO_2 **	2.3
Total 3	3.6

* Assuming 1 mil x 2 mil films

** Assuming a 6 mil thick substrate

Table 1 Comparison of heat flows in μW for a 2 mil spacing

Lead Assembly	% Reduction in Thermal Loss of the Lead Wires	% Thermal Savings for the System	Lifetime Extension (5 yr mission)	Lifetime Extension (7 yr mission)
123/Fused Silica				
Model 1	70.5%	11.4%	6.9 months	9.6 months
Model 2	80.7%	13.2%	7.9 months	11.1 months
2223/Fused Silica				
Model 1	77.7%	12.7%	7.6 months	10.6 months
Model 2	87.9%	14.4%	8.6 months	12.1 months
123/Cubic YSZ				
Model 1	15.8%	2.1%	1.3 months	1.8 months
Model 2	53.4%	8.5%	5.1 months	7.2 months
2223/Cubic YSZ				
Model 1	23.0%	3.4%	2.0 months	2.8 months
Model 2	60.6%	9.8%	5.9 months	8.2 months

Table 2 Calculated heat flows through candidate high-Tc superconductive lead assemblies (per lead basis)

Lead Assembly	Heat Flow (μW) - Model 1	Heat Flow (μW) - Model 2
123/Fused Silica	4.9	3.2
2223/Fused Silica	3.7	2.0
123/Cubic YSZ	14	7.8
2223/Cubic YSZ	12.8	6.6
Manganin	**16.6**	**16.6**
123/Alumina	883.5	442.5
2223/Alumina	882.3	441.3
123/Magnesia	8020.5	4011.5
2223/Magnesia	8019.3	4010.3

Table 3 Estimates thermal savings using various lead assemblies.